

# A New Approach for Multistage Analog Complex Filter Design

Daniele Grasso, Giuseppe Avellone

Automotive Product Group - Radio Frequency Competence Center

STMicroelectronics

Catania, Italy

daniele.grasso@st.com, giuseppe.avellone@st.com.

**Abstract**— In this paper, a design approach for  $g_m$ -C complex filter for intermediate frequency (IF) is formalized. It is based on decoupled first order  $g_m$ -C sections, each one centered at a different frequency with respect to the others that can be stacked in series to get the final band pass filter response, with order equal to the number of stages. A simple case with two stages is presented to show selectivity improvement when difference between the two center-bands increase, with ripple increase as drawback. An optimal setup with good selectivity increment and still zero ripple (flat pass-band) is also shown. Then, the approach is extended to third order. The approach has been used for IF filtering in STMicroelectronics GNSS receivers, but it is applicable to other wireless receivers.

**Keywords**-  $g_m$ -C filter, complex filtering, low-IF receivers.

## I. INTRODUCTION

The complex intermediate frequency (IF) filters have been proposed for radio frequency (RF) front-end (especially for the low-IF ones) for their characteristic of rejecting both out-of-band and image signals, due to their asymmetrical transferring function [1]. Several implementations have been disclosed in technical literature, such as [1]-[8], mainly based on active circuits, while related impairments has been also analyzed in [9] and the references therein. Amongst these implementations, it has been chosen the one based on decoupled first order stacked stages with operational trans-conductor amplifier (OTA) and frequency shift of low-pass prototype. This choice presents lower current consumption, good response at high frequency and simple, reconfigurable, modular design [10].

In the state-of-the-art implementation of  $g_m$ -C multistage complex IF filter, each stage is centered on the same frequency with the same bandwidth, as in [1], [4] and [15] and the references therein. In this contribution, we formalize an approach considering different center frequency for each stage (and eventually different bandwidth). These center frequencies will be placed symmetrically around the center frequency of the final filter. This approach achieves better performances, especially in terms of out-of-band attenuation, image rejection and flatness in group delay response with lower current consumption (as shown in [10]). Moreover, it allows more freedom in shaping the filter frequency response for a given filter order. We adopted it in designing an IF filter for Global Navigation Satellite Systems (GNSS) receivers described in [10]-[12].

Section II describes the complex IF filter architecture, as in [10]; Section III presents the proposed approach considering the second order complex filter case, providing equations for filter design, and comparing the behavior between coincident center and non-coincident center cases. Section IV gives a brief extension to third order, and the main conclusions are drawn in Section V.

## II. COMPLEX FILTER ARCHITECTURE

Filter architecture is based on decoupled first order sections stacked in series to get the final band-pass filter order. Each single stage band-pass filter response is a frequency shifted version of a low-pass one, designed using active components with trans-conductors and capacitors ( $g_m$ -C or OTA-C). Fig. 1 shows the architecture used in [10]-[12] for the single-stage, where the first order low-pass frequency response is set by the OTA  $g_{m1}$  and capacitor  $C$  values, with bandwidth given by:  $f_{LP} = (g_{m1}/2\pi C)$ . The structure with the  $g_{m2}$  OTA is a gyrator that creates a feedback between in-phase (I) and quadrature (Q) branches performing the frequency shift of the low-pass prototype response, obtaining a band-pass centered at a frequency defined through  $g_{m2}$  and  $C$  values according to the formula:  $f_{center} = (g_{m2}/2\pi C)$ . The transfer function can be obtained just putting the translation

$$j\omega \rightarrow j\omega - j\omega_{center} \quad (1)$$

in the transfer function of the low pass version, [1],[13]-[14]:

$$H_{LP}(j\omega) = \frac{G}{1 + j\omega/\omega_{LP}} \quad (2)$$

resulting in

$$H_{BP}(j\omega) = \frac{G}{1 + j(\omega - \omega_{center})/\omega_{LP}} \quad (3)$$

with  $G = (g_{m3}/g_{m1})$ , where the third OTA,  $g_{m3}$ , is used both to decouple each stage with the previous one and to provide a gain (as a free parameter).

In [10], we performed several schematic level simulations for defining design parameters values as a better trade-off amongst requirements of bandwidth, in-band group-delay variation, image and out-of-band rejection. We considered a 3<sup>rd</sup> or 4<sup>th</sup> order filter comparing in detail two cases:

- stages with same center frequency and bandwidth;
- stages with different center frequencies, same bandwidth.

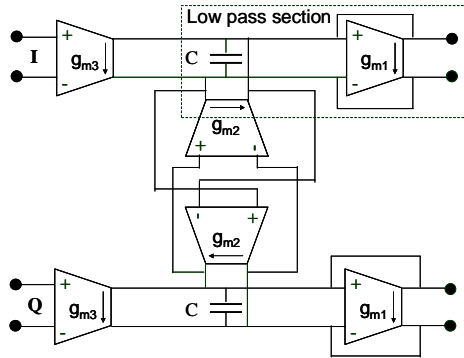


Figure 1. Complex filter single-stage basic architecture.

It was easily recognizable as the second case presents better performances, especially in terms of out-of-band attenuation, image rejection and flatness in group delay response. In fact, in [10], we have observed that, when all stages share the same center frequency, if wider bandwidth are needed with low-order filters, the properties of both out-of-band and image rejection rapidly becomes not acceptable. On the contrary, the different center frequency configuration can achieve wider bandwidth while maintaining low-order IF filter with good rejection for both out-of-band and image signals. The drawback of this latter approach is that the implementation needs different gyrators, one for each stage, instead of only one type for all the stages. Once fixed the stages main parameters ( $f_{center}$ ,  $f_{LP}$  and  $G$ ), then  $g_{m1}$ ,  $g_{m2}$  and  $g_{m3}$  are fixed from the previous formulas and all the transconductors can be designed. For the details of the circuit design and measurement results, see [10]-[12].

### III. COMPLEX FILTER FORMALIZATION

To formalize what has been observed both by simulation and by measurements on the implemented IF filters, it is better to take into account a simplified version with only two stages, obtaining a second order filter (but the approach and the conclusions can be straightforwardly extended to higher order complex analog filters). In this case, the transfer function for two equal stages is

$$H_C(j\omega) = \frac{G^2}{\left(1 + j \frac{\omega - \omega_{center}}{\omega_{LP}}\right)^2}. \quad (4)$$

Meanwhile, for two stages with centers respectively in  $\omega_{center1}$  and  $\omega_{center2}$  is

$$\begin{aligned} H_{NC}(j\omega) &= H_{BP1}(j\omega) \cdot H_{BP2}(j\omega) = \\ &= \frac{G}{1 + j \frac{\omega - \omega_{center1}}{\omega_{LP}}} \cdot \frac{G}{1 + j \frac{\omega - \omega_{center2}}{\omega_{LP}}}. \end{aligned} \quad (5)$$

For a final pass-band filter centered at  $\omega_{center}$  and band equal to  $2\omega_B$ ,  $\omega_{center1}$  and  $\omega_{center2}$  must be chosen symmetrical to  $\omega_{center}$ , that is  $\omega_{center} = (\omega_{center1} + \omega_{center2})/2$ . Normalizing all the frequencies with respect to  $\omega_B$ , (4) and (5) become:

$$H_C(j\omega_n) = \frac{G^2}{\left(1 + j \frac{\omega_n - \omega_c}{\omega_o}\right)^2} \quad (6)$$

$$H_{NC}(j\omega_n) = \frac{G^2}{\left(1 + j \frac{\omega_n - \omega_{c1}}{\omega_o}\right) \cdot \left(1 + j \frac{\omega_n - \omega_{c2}}{\omega_o}\right)} \quad (7)$$

where  $\omega_n = \omega/\omega_B$ ,  $\omega_c = \omega_{center}/\omega_B$ ,  $\omega_o = \omega_{LP}/\omega_B$ ,  $\omega_{c1} = \omega_{center1}/\omega_B$ ,  $\omega_{c2} = \omega_{center2}/\omega_B$ , and the normalized filter bandwidth is 2. In the same way the upper 3dB corner of the band is  $\omega_c + 1$  and the lower is  $\omega_c - 1$ .

#### A. Coincident Center Frequency Case

Without losing general validity, we set  $|H_{coinc}(j\omega_c)| = 1$ , this lead to  $G=1$ . Now, we want calculate the single stage low-pass normalized band  $\omega_b$  needed for a final normalized bandwidth equal to 2 of the two stages filter. This happens when the magnitude at the normalized upper band corner  $\omega_c + 1$  is 3dB lower than the center-band one, that is:

$$\frac{|H_C[j(\omega_c + 1)]|}{|H_C[j(\omega_c)]|} = \frac{1}{\sqrt{2}}; \quad (8)$$

considering (6), condition (8) is verified for  $\omega_b = 1.554$ .

This means that in order to have a two coincident stages band-pass filter with bandwidth of  $2\omega_B$  we need a low pass bandwidth of  $1.554 \cdot \omega_b$  for each single stage.

#### B. Different Center Frequency Case

Setting  $\omega_d = (\omega_{c2} - \omega_{c1})/2$ , then  $\omega_{c1} = \omega_c - \omega_d$  and  $\omega_{c2} = \omega_c + \omega_d$ , and equation (7) may be written as:

$$\begin{aligned} |H_{NC}(j\omega_n)|^2 &= \\ &= \frac{G^4 \omega_o^4}{(\omega_n - \omega_c)^4 + 2(\omega_o^2 - \omega_d^2)(\omega_n - \omega_c)^2 + (\omega_d^2 + \omega_o^2)^2} \end{aligned} \quad (9)$$

Analyzing this function it is possible to distinguish two cases:

- if  $\omega_d < \omega_o$  then the filter frequency response has only one maximum (MAX) at  $\omega_n = \omega_c$  equal to

$$MAX = |H_{NC}(j\omega_c)| = G^2 \omega_o^2 / (\omega_d^2 + \omega_o^2) \quad (10)$$

- if  $\omega_d > \omega_o$ , then the filter frequency response has one minimum (min) at  $\omega_n = \omega_c$  equal to

$$\min = |H_{NC}(j\omega_c)| = G^2 \omega_o^2 / (\omega_d^2 + \omega_o^2) \quad (11)$$

and two equal maximum values at

$$\omega_n = \omega_{MAX} = \omega_c \pm \sqrt{\omega_d^2 - \omega_o^2} \quad (12)$$

both with value

$$\text{MAX} = \left| H_C \left[ j(\omega_c \pm \sqrt{\omega_d^2 - \omega_o^2}) \right] \right| = G^2 \omega_o / 2\omega_d \quad (13)$$

Considering the first case, we want to calculate, also for non-coincident center, the single stage low-pass normalized band needed for a final normalized bandwidth equal to 2 for the two-stage filter. In general, we obtain a different value respect the one calculated in section A; for this reason, let put  $\omega'_o$  instead of  $\omega_o$  to distinguish the new variable. Further, we set  $|H_{NC}(j\omega_c)| = 1$  obtaining from (9)

$$G^2 = (\omega_d^2 + \omega_o'^2) / \omega_o'^2 \quad (14)$$

and

$$\begin{aligned} |H_{NC}(j\omega_n)| &= \\ &= \frac{\omega_d^2 + \omega_o'^2}{\sqrt{(\omega_n - \omega_c)^4 + 2(\omega_o'^2 - \omega_d^2)(\omega_n - \omega_c)^2 + (\omega_d^2 + \omega_o'^2)^2}} \end{aligned} \quad (15)$$

Then, setting (8) for 3dB cut off at  $\omega_c + 1$  we obtain:

$$\omega_o'^2 = 1 - \omega_d^2 \pm \sqrt{\omega_d^4 - 4\omega_d^2 + 2} \quad (16)$$

These are valid when  $0 \leq \omega_d \leq \sqrt{2 - \sqrt{2}}$ ; and  $\omega_d \geq \sqrt{2 + \sqrt{2}}$ ; the plot of (16), '+' case, results as in Fig. 2: all the negative values are not acceptable, so we can discard the values for  $\omega_d \geq \sqrt{2 + \sqrt{2}}$ . Furthermore, we must discard the solutions not compliant with  $\omega_d < \omega'_o$ ; plotting the square root of (16), it is easy to verify that only the solutions for  $0 \leq \omega_d \leq 0.7596$  can be considered. Other solutions of (16) can be found in the '-' case, but the condition  $\omega_d < \omega'_o$  is never satisfied and cannot be considered. So, final solution in  $\omega_d < \omega'_o$  case is

$$\omega'_o = \sqrt{1 - \omega_d^2 + \sqrt{\omega_d^4 - 4\omega_d^2 + 2}} \quad (17)$$

true for  $0 \leq \omega_d \leq 0.7596$ . Fig. 3 shows the needed low-pass bandwidth of each stage versus frequency distance of the responses of the two stages. Observing this plot, for  $\omega_d = 0$  we should have the previous coincident center case, and in fact we found the previous value  $\omega'_o = \omega_o = 1.554$ ; when  $\omega_d$  increases then  $\omega'_o$  decreases: this means that each stage can have a narrower bandwidth for obtaining the desired resulting bandwidth of the whole two-stage filter, that is a normalized value equal to 2. This lead to higher slope of the out-of-band response, that is higher out-of-band attenuation with the same bandwidth, so it is possible to obtain a more selective filter. Just to make an example, choosing  $\omega_d = 0.7$ , we obtain  $\omega'_o = 1.0194$ , less than  $\omega_o = 1.554$  in the coincident center case also satisfying condition:  $\omega_d < \omega'_o$ .

In order to evaluate the selectivity improvement, the out-of-band attenuation can be calculated anywhere for both cases, e.g. in  $\omega_c + 10$ . For not coincident case from (15), substituting  $\omega_d = 0.7$  and  $\omega'_o = 1.0194$ , we have

$$A_{NC}(\omega_c + 10) = 36.4 \text{ dB} \quad (18)$$

for coincident center case, from (6), (8) and  $G = 1$ , we have

$$A_C(\omega_c + 10) = 32.5 \text{ dB} \quad (19)$$

with 3.9dB of more attenuation in the not coincident case, resulting in more selectivity as both have same normalized bandwidth equal to 2.

Choosing another value of out-band frequency, nearer the band of the filter, for example  $\omega_c + 3$ , we have

$$A_{NC}(3) - A_C(3) = 16.0 - 13.5 = 2.5 \text{ dB} \quad (20)$$

and that confirms the selectivity enhancement.

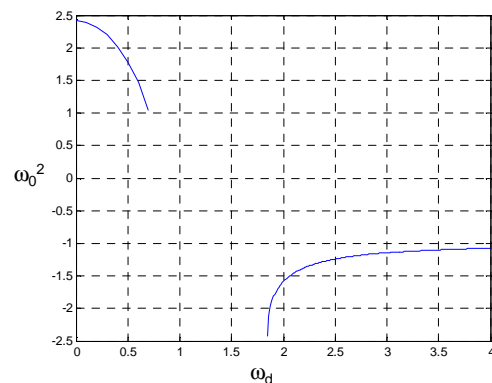
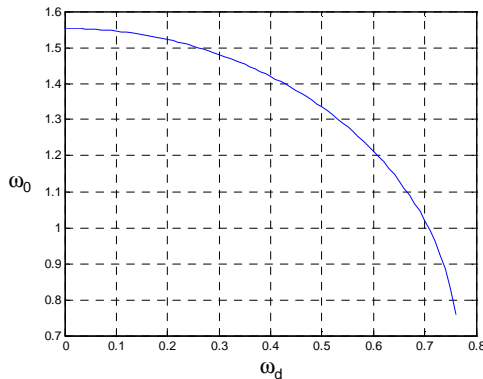


Figure 2. Plot of Eq. 16, plus case, for the allowed values of  $\omega_d$ .


 Figure 3. Plot of Eq. 17, for the allowed values of  $\omega_d$ .

Now, let's consider  $\omega_d > \omega'_o$ , still with not-coincident center, and set the values of the two peaks equal to MAX=1 without losing general validity, so from (13) is

$$G^2 = 2\omega_d/\omega'_o \quad (21),$$

and (9) becomes

$$|H_{NC}(j\omega_n)|^2 = \frac{4\omega_d^2\omega'^2_o}{(\omega_n - \omega_c)^4 + 2(\omega'^2_o - \omega_d^2)(\omega_n - \omega_c)^2 + (\omega_d^2 + \omega'^2_o)^2} \quad (22)$$

Then, once again, we impose a normalized bandwidth of the resulting filter equal to 2; this means that in  $\omega_c \pm 1$  the response must be  $1/\sqrt{2}$  times the maximum. From (22) imposing the condition (8) we obtain:

$$\omega'_o = \sqrt{3\omega_d^2 - 1 \pm 2\omega_d\sqrt{2\omega_d^2 - 1}} \quad (23)$$

valid for  $\omega_d \geq 1/\sqrt{2}$ . The plot of (23) results as in Fig. 4: as easily recognizable the '+' case (dashed line) does not match the condition  $\omega_d > \omega'_o$ , so can be discarded. Observing the '-' case (continuous line) is possible to split the curve in two parts: the first one, on which we focus our interest, with decreasing value of  $\omega'_o$  for  $1/\sqrt{2} \leq \omega_d < 1$ , up to  $\omega_d = 1$ , that means when the center frequency separation of the two stage is equal to the bandwidth of the whole filter. In this point the  $\omega'_o$  required is zero, so it is only a theoretical limit. The second part for  $\omega_d > 1$ , that is center frequency separation of the two stages greater than the bandwidth of the whole filter, lacks of interest because the response of each stage is completely separated from the other, so not useful to obtain an appropriate overall pass-band response.

Returning to the range  $1/\sqrt{2} \leq \omega_d < 1$  in (23), as noted before, the decreasing characteristic of  $\omega'_o$  suggests more

selective behavior for higher  $\omega_d$ ; further, the presence of two peaks, as formalized in (11), (12) and (13), means presence of in-band ripple: when  $\omega_d$  increases, the minimum in  $\omega_c$  becomes lower and the ripple increases. It is important to check when ripple is too big.

If the difference between maximum and minimum becomes greater than 3dB then we can consider the response completely separated into two distinct lobes, non-acceptable as band-pass characteristic. The limit of the center frequencies separation  $\omega_d$  that still gives us a unique filter band is given for ripple equal to 3dB, that is:

$$F(\omega_d) = \frac{|H_{NC}[j(\omega_c)]|}{|H_{NC}[j(\omega_{MAX})]|} = \frac{1}{\sqrt{2}} \quad (24)$$

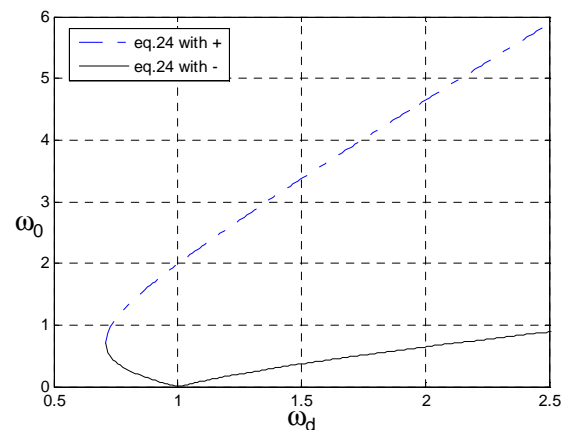
Considering the (21) and the (22) then is

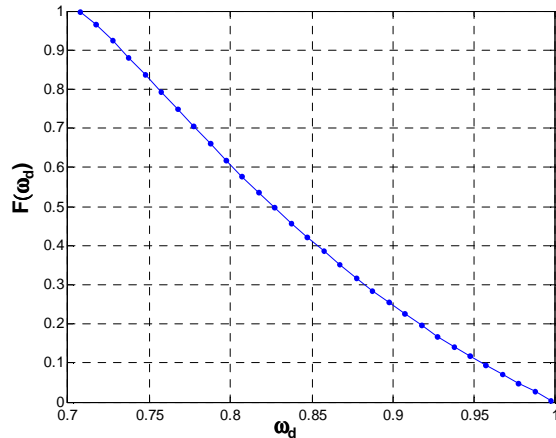
$$F(\omega_d) = 2\omega_d\omega'_o/(\omega'^2_o + \omega_d^2) \quad (25)$$

where  $\omega'_o$  has the value for a final band equal to 2, given by (23) for  $1/\sqrt{2} \leq \omega_d < 1$ ; substituting it we have:

$$F(\omega_d) = \frac{2\omega_d(\omega_d - \sqrt{2\omega_d^2 - 1})}{4\omega_d^2 - 2\omega_d\sqrt{2\omega_d^2 - 1} - 1} \quad (26)$$

Plotting (26) (see Fig. 5) the condition in (24) is satisfied for  $\omega_d = 0.77679$ ; this value gives the maximum acceptable ripple. Observing the same plot is fine to note that for  $\omega_d = 1/\sqrt{2}$  we found  $F(\omega_d)=1$ . This is the case with no ripple, because the minimum is equal to the two maximum values, and coincides with the case previously studied for  $\omega_d < \omega'_o$  having only one maximum, where we observed that higher  $\omega_d$  brings to higher selective filter.


 Figure 4. Plot of Eq. 23, for the allowed values of  $\omega_d$ .


 Figure 5. Plot of Eq. 26, for the allowed values of  $\omega_d$ .

So, choosing  $\omega_d = 1/\sqrt{2}$  gives the resulting filter with higher selectivity and no ripple; if we can accept ripple, we can choose a greater value of  $\omega_d$  in the range  $1/\sqrt{2} \leq \omega_d \leq 0.77679$ . In particular we can choose values nearer to 0.77679 for better selectivity despite of worse ripple. If for example we choose  $\omega_d = 0.77$  from (23), ' case, we have  $\omega'_0 = 0.3389$ , very low compared with the one of the best values we can have for  $\omega_d < \omega'_0$ , for example for  $\omega_d = 0.7$  from (16) we already found  $\omega'_0 = 1.0194 \gg 0.3389$ ; in this way, with so low  $\omega'_0$ , we have much more selectivity. If we compare it with the coincident center case, the difference is even bigger (from (9) it was  $1.554 \gg 0.3389$ ). Evaluating the attenuation in the same out-of-band frequencies used in the examples in all the previous cases we obtain the values in Table I.

Another interesting example can be considered for the "optimum" setup that gives maximum out-of-band attenuation with still zero ripple. As already discussed, it is for  $\omega_d = 1/\sqrt{2}$  in  $\omega_d \geq \omega'_0$  case, and for about  $\omega_d = 0.7596$  in  $\omega_d < \omega'_0$  case. The values of  $\omega'_0$  are  $1/\sqrt{2}$  and 0.7622 respectively, while the related attenuations for  $\omega_c+3$  and  $\omega_c+10$  are in Table II. In both cases, the maximum attenuation with zero ripple is when the two-stages frequency separation,  $\omega_d$ , is equal to the single stage bandwidth  $\omega'_0$ .

TABLE I. COMPARISON OF OUT-OF-BAND ATTENUATIONS AMONGST NON COINCIDENT FREQUENCIES CASES AND COINCIDENT FREQUENCIES

|               | Ripple $\omega_d=0.77$ | No ripple $\omega_d=0.7$ | Equal Freq.     |
|---------------|------------------------|--------------------------|-----------------|
| $\omega_c+3$  | $A_{NC} = 24.3$ dB     | $A_{NC} = 16.0$ dB       | $A_C = 13.5$ dB |
| $\omega_c+10$ | $A_{NC} = 45.6$ dB     | $A_{NC} = 36.4$ dB       | $A_C = 32.5$ dB |

TABLE II. MAXIMUM OUT-OF-BAND ATTENUATION WITH NO RIPPLE

|               | No ripple $\omega_d \geq \omega'_0$ | No ripple $\omega_d < \omega'_0$ |
|---------------|-------------------------------------|----------------------------------|
| $\omega_c+3$  | $A_{NC} = 19.1$ dB                  | $A_{NC} = 17.9$ dB               |
| $\omega_c+10$ | $A_{NC} = 40.0$ dB                  | $A_{NC} = 38.7$ dB               |

Lastly, maximum selectivity, with 3dB ripple, is for  $\omega_d = 0.77679$ , obtaining  $A_{NC}(\omega_c+3) = 24.6$  dB and  $A_{NC}(\omega_c+10) = 46.0$  dB.

#### IV. THIRD ORDER CASE

In this section, we will give a brief look to the third order case. For three stages with normalized centers, respectively, in  $\omega_{c1}$ ,  $\omega_{c2}$  and  $\omega_c$  the transferring function is

$$H_{NC}(j\omega_n) = \frac{K}{\left(1 + j \frac{\omega_n - \omega_{c1}}{\omega_o}\right) \cdot \left(1 + j \frac{\omega_n - \omega_{c2}}{\omega_o}\right) \left(1 + j \frac{\omega_n - \omega_c}{\omega_o}\right)} \quad (27)$$

where  $K = G_1 G_2 G_3$  is the filter gain,  $\omega_n = \omega/\omega_B$ ,  $\omega_c = \omega_{center}/\omega_B$ ,  $\omega_{c1} = \omega_{center1}/\omega_B$ ,  $\omega_{c2} = \omega_{center2}/\omega_B$ ,  $\omega_o = \omega_{LP}/\omega_B$  and the normalized filter bandwidth is 2. Moreover,  $\omega_{c1}$  and  $\omega_{c2}$  must be chosen symmetrical to  $\omega_c$ , that is  $\omega_c = (\omega_{c1} + \omega_{c2})/2$ . Setting  $\omega_d = (\omega_{c2} - \omega_{c1})/2$ , then  $\omega_{c1} = \omega_c - \omega_d$  and  $\omega_{c2} = \omega_c + \omega_d$ , equation (27) may be written as

$$H_{NC}(j\omega_n) = \frac{K}{\left(1 + j \frac{\omega_n - \omega_c + \omega_d}{\omega_o}\right) \cdot \left(1 + j \frac{\omega_n - \omega_c - \omega_d}{\omega_o}\right) \left(1 + j \frac{\omega_n - \omega_c}{\omega_o}\right)} \quad (28)$$

Setting  $x = (\omega_n - \omega_c)$  and developing denominator in (28) we obtain:

$$H_{NC}(j\omega_n) = \frac{K\omega_o^3}{[\omega_o(\omega_o^2 - 3x^2 + \omega_d^2) + jx(3\omega_o^2 - x^2 + \omega_d^2)]} \quad (29)$$

The square modulus becomes:

$$|H_{NC}(j\omega_n)|^2 = \frac{K^2\omega_o^6}{[\omega_o^2(\omega_o^2 - 3x^2 + \omega_d^2)^2 + x^2(3\omega_o^2 - x^2 + \omega_d^2)^2]} \quad (30)$$

Maximum and minimum values will be related to minimum and maximum values of denominator in (30). So, let us consider the derivate of the denominator with respect to  $x$  equating it to zero (defining for which  $x$  there could be maximum and minimum values):

$$6x^5 + 4x^3(3\omega_o^2 - 2\omega_d^2) + 2x(3\omega_o^2 + \omega_d^2) = 0 \quad (31)$$

The first solution is  $x=0 \Rightarrow \omega_n = \omega_c$ ; other solutions from:

$$x^4 + \frac{2}{3}x^2(3\omega_o^2 - 2\omega_d^2) + \frac{1}{3}(3\omega_o^2 + \omega_d^2) = 0 \quad (32)$$

setting  $x^2=y$ , solution of (32) has the following expressions:

$$y_{1,2} = -\frac{1}{3}(3\omega_o^2 - 2\omega_d^2) \pm \frac{1}{3}\omega_d\sqrt{\omega_d^2 - 12\omega_o^2} \quad (33)$$

Solutions (33) are real for  $\omega_d^2 \geq 12\omega_o^2$ . If this last holds, these are acceptable solutions for  $x$  if and only if  $y_{1,2} \geq 0$ . In this latter case, both solutions are non-negative; so there are two couples of frequencies to be considered:

$$\begin{aligned}\omega_{n1} &= \omega_c \pm \sqrt{y_1} \\ \omega_{n2} &= \omega_c \pm \sqrt{y_2}\end{aligned}\quad (34)$$

On the contrary, if  $y_{1,2} < 0$ , there will be only one real solution for (33) and for  $\omega_i = \omega_c$  the transfer function present only a maximum and no ripple:

$$|H_{NC}(j\omega_c)|^2 = \frac{K^2 \omega_0^4}{(\omega_0^2 + \omega_d^2)^2}. \quad (35)$$

Considering  $y_{1,2} \geq 0$  for the frequencies in (34), the transfer function presents more solutions. In this case, we can have three maxima (one always from (35)) and two minima, and ripple will be present as in Fig. 6.

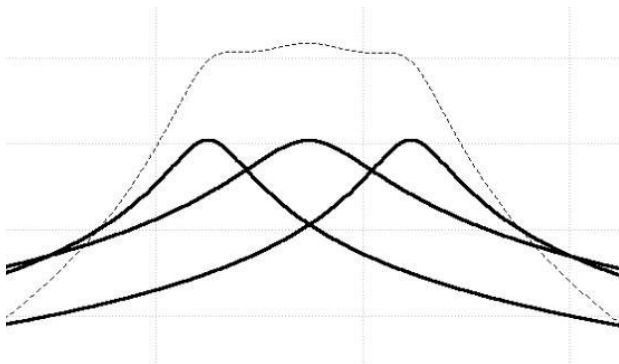


Figure 6. Third order complex filter transfer function (dot) and transfer function of each first order stage.

For this case, we have to verify both that  $\omega_i = \omega_c + l$  is cut-off frequency and the in-band ripple; imposing the maximum value for this last parameter in order to verify if there are acceptable solutions for  $\omega_0$  and  $\omega_d$ . For instance, for  $\omega_d^2 = 12\omega_0^2$  the ripple is not acceptable. Moreover, it can be observed that the selectivity increases as a function of  $\omega_d$ .

## V. CONCLUSIONS AND FUTURE WORK

We have described an approach for multistage complex IF filter design able to reach a good tradeoff between in-band ripple and rejection of both out-of-band and image frequency using different center frequencies in each stage, also choosing properly their bandwidths. Formulas are also provided for the filter design in the two stages case, obtaining the desired selectivity and ripple just choosing the bandwidth and the center frequency of each stage. We have also briefly described the third order case and extension to higher order is quite straightforward. We have adopted this approach for IF filter design in STMicroelectronics GNSS receiver, [10]-[12].

Future work could be the extension of the proposed approach to design filter where each stage shows different order, bandwidth and center frequency asymmetrically placed respect to the center of the passband.

## ACKNOWLEDGMENT

The authors are grateful to Angela Bruno for support, discussions and helpful advices.

## REFERENCES

- [1] K.W. Martin, "Complex signal processing is not complex", IEEE Trans. on Circ. and Syst. I: Regular Papers, vol.51, no.9, pp.1823,1836, Sept. 2004
- [2] P. Khumsat and A. Worapishet, "5th-order Chebyshev Active-RC Complex Filter Employing Current Amplifiers", Proc. IEEE Int. Symp. on Integrated Circuit, Sept. 26-28, 2007, pp. 281-284, Singapore.
- [3] V. Della Torre, M. Conta, R. Chokkalingam, G. Cusmai, P. Rossi, and F. Svelto, "A 20 mW 3.24 mm2 Fully Integrated GPS Radio for Location Based Services", IEEE J. of Solid-State Circuits, vol. 42, no. 3, March 2007, pp. 602-612.
- [4] L. Laccisaglia, "Progetto di un filtro passa banda per segnali I-Q in un ricevitore a low-IF per applicazione GPS in tecnologia CMOS" Master Thesis, Rome University "La Sapienza", 2004.
- [5] F. Behbahani, H. Firouzkouhi, R. Chokkalingam, S. Delshadpour, A. Kheirkhahi, M. Nariman, et al., "A 27mW GPS Radio in 0.35 $\mu$ m CMOS", Proc. IEEE Int. Solid-State Circ. Conf., vol.1, Feb. 3-7, 2002, pp. 398-476, San Francisco.
- [6] C-W Chen, Y-C Chung, O. T-C. Chen, and R.Y.J. Tsen, "A Concurrent L1 and L2-band GPS Receiver Using an Integrated Low-IF and Weaver Architecture", Proc. IEEE Int. Symp. on Micro-NanoMechatronics and Human Science, Dec. 27-30, 2003, vol.3, pp. 1163-1166.
- [7] A. Abuelma'atti and M.T. Abuelma'atti, "A new active polyphase filter for image rejection using second generation current conveyors", Proc. 9<sup>th</sup> WSEAS Int. Conf. on Circuits, July 11-13, 2005, Athens, Greece.
- [8] H. Kondo, M. Sawada, N. Murakami, S. Masui, M. Fujioka, K. Maruyama, M. Naganuma, and H. Fujiyama, "Complex BPF for Low-IF receivers with an Automatic Digital Tuning Circuit", RFIT2007-IEEE Int. Workshop on Radio-Frequency Integration Technology, Dec. 9-11, 2007, pp.74-77, Singapore.
- [9] J. Mahattanakul, "The effect of I/Q imbalance and complex filter component mismatch in Low-IF receivers", IEEE Trans. on Circ. and Syst. I: Regular Papers, vol. 53, no. 2, Feb. 2006, pp. 247-253.
- [10] D. Grasso, G. Avellone, G. Rivela, G. Calí, and S. Scaccianoce, "An Adaptive Low-Power Complex gm-C IF Filter for L1/E1 GPS/Galileo Signals", IEEJ Int. Analog VLSI Workshop, AVLSIWS 2010, Sept. 8-10, 2010, Pavia, Italy.
- [11] G. Rivela, P. Scavini, D. Grasso, A. Calcagno, M. Castro, G. Di Chiara, G. Avellone, G. Calí, and S. Scaccianoce, "A 65 nm CMOS Low Power RF Front-End for L1/E1 GPS/Galileo Signals", Great Lake Symposium on VLSI, GLSVLSI, May 2-4, 2011, Lausanne, Switzerland.
- [12] G. Rivela, P. Scavini, D. Grasso, M. Castro, A. Calcagno, G. Avellone, A. Di Mauro, G. Calí, and S. Scaccianoce, "A low power RF front-end for L1/E1 GPS/Galileo and GLONASS signals in CMOS 65nm technology," Localization and GNSS Int. Conf. on , ICL-GNSS, June 29-30, 2011, pp.7-12.
- [13] C. Cuypers, N.Y. Voo, M. Teplechuk, and J.I. Sewell, "General synthesis of complex analogue filters", IEE Proc. Circuits, Dev. and Syst., vol. 152, no. 1, Feb. 2005, pp.7-15.
- [14] S. Hintea, G. Csipkes, C. Rus, D. Csipkes, and H. Fernandez-Canque, "On the Design of a Reconfigurable OTA-C Filter for Software Radio", IEEE 2<sup>nd</sup> NASA/ESA Conf. on Adaptive Hardware and Systems (AHS 2007), Aug. 5-8, 2007, pp. 541-546, Edinburgh.
- [15] H. Liu, Z. Fu, F. Lin, "A Low Power Gm-C Complex Filter for ZigBee Receiver", IEEE Microwave and Millimeter Wave Technology (ICMMT 2012) Int. Conf. on, May 5-8, 2012, pp.1-4, Shenzhen, China.